Egyptian Geophysical Society
EGS Journal, Vol. 16, No. 1, 97-110 (2018)

SUB-SALT SEISMIC IMAGE ENHANCEMENT USING 3D PRE-STACK DEPTH CONTROLLED BEAM MIGRATION -RASBUDRAN FIELD, CENTRAL PROVINCE OF THE GULF OF SUEZ, EGYPT

A.K. EL-WERR, A. EL-RAWY, A. GADALLAH and M.S. EL-HATEEL

Geophysics Dept., Faculty of Science, Ain Shams University, Cairo, Egypt.

تحسين التصوير السيزمى للطبقات تحت الملحية باستخدام تصحيح العمق ثلاثى الأبعاد ما قبل التجميع لحزمة الأشعة المتحكمة- حقل رأس بدران – وسط خليج السويس – مصر

الخلاصة: يفرض الوضع الجيولوجي المعقد لخليج السويس تحديات للتصوير السيزمى. حيث أنه يحتوى جيولوجيا على الميوسين العلوى – ممثلا بمكون زيت الذى يتكون من طبقات طفلية منخفضة السرعة مع تداخلات من طبقات متبخرات من الملح والأنهيدريت عالية السرعة التى تسبب الكثير من المضاعفات الانعكاسية، بالإضافة إلى وجود العديد من الكتل الصدعية المائلة والتى تسبب تغييرا جانبيا كبيرا في سرعة الموجات السيزمية. ووجود هذه الطبقات عالية السرعة داخل القطاع الرسوبي في خليج السويس يعزز معامل الانعكاس على طول الأسطح الفاصلة بينها وبالتالي تظهر واضحة على أبواب القطاعات السيزمية. ونتيجة لذلك تختفى الأسطح الانعكاسية المفيدة لأي وحدة صخرية تحت هذه المتبخرات بشكل واضح. وهذا بدوره يؤدي إلى نشأة صعوبة التصوير الانعكاسى لما قبل الملح نظرا للاختلافات الكبيرة فى السرعة الجانبية ، وتشويه مسارات الأشعة وسحب أزمنة أسطح هذه الطبقات لأعلى بسبب وجود الملح ذات السرعة العالية. تتناول هذه الدراسة التصوير السيزمى فى العمق للتراكيب العميقة تحت هذا الغطاء المعقد والتى تظهر اختلافات فى السرعة الأفقية والرأسية. فى مثل هذه الأماكن دائما ما يعانى التصوير السيزمى من انخفاض فى جودة البيانات ووجود نماذج كاذبة للطبقات العميقة ناتجة من اضطراب فى انتشار الموجات السيزمية خلال الطبقات العليا المشوهة. وتتأثر القطاعات السيزمية لتصحيح العمق فى الزمن ما قبل التجميع بقوة أنشطة الانعكاسات المتعددة و فقدان معظم الطاقة السيزمية بسبب المشاكل المذكورة أعلاه. وبالتالى تم استخدام تصحيح العمق ما قبل التجميع فى العمق ثلاثى الأبعاد لتحسين لتصوير السيزمى للطبقات ما قبل الملح فى حقل بترول رأس بدران وسط خليج السويس.

ABSTRACT: *The geological nature of the Gulf of Suez has a complex geological setting that poses challenges for seismic imaging.Geologically the Gulf of Suez contains the Upper Miocene - Zeit Formation with low velocity shaley beds and high velocity of salt and anhydrite beds that causes a lot of multiples. In addition, the presence of several tilted fault blocks results in big lateral change in velocity. The presence of high velocity layers like Miocene salts and anhydrites within the sedimentary sequence in the Gulf of Suez enhances the reflection coefficient along their interfaces with consequently apparent resolution of these horizons on seismic sections. As a result, the absence of any beneficial seismic reflection horizons of any rock unit below this evaporite section is clearly observed. That is in turn, leads to difficulty of imaging the pre-salt reflectors due to the significant lateral velocity variations, distortion of raypaths and time pull-up created by salt. The present study discusses the depth seismic images of the deep structural objectives beneath a complex overburden that may show strong horizontal and vertical velocity variations. In such areas, the seismic image is frequently of poor quality and the depth model of deep layers is often false due to the perturbed propagation of seismic energy through the deforming effect of the overlying layers. This complexity of the geologic section makes seismic processing and interpretation being a big challenge for geophysicists. Hence, planning and drilling new wells are so difficult due to unexpected events, i.e. faults, missing targets etc. Several interpretations based on the 2D and 3D seismic were performed in the Ras Budran study area. Pre-stack time migration (PSTM) seismic sections are strongly affected by multiple activities and heavy seismic energy loss due to the problems mentioned above. Hence, 3D pre-stack depth migration with a controlled beam migration algorithm was used to enhance the sub-salt seismic imaging at Ras Budran oil field, central province of the Gulf of Suez.*

INTRODUCTION

RasBudran oil field study area is one of the Gulf of Suez fields which are located in the central province of the eastern coast of the Gulf of Suez, where the dip regime of the pre-Miocene is to the northeast. It lies in the north of Belayim offshore concession area, approximately 4 km west to Sinai coast of Gulf of Suez and 13 km northwest of Abu Rudeis city.RasBudran field is bounded by six corners (1-6) with co-ordinates as follows: 1- Latitude: 28° 57' 0.533" N, Longitude 33° 9' 6.047" E, 2- Lat: 28° 57' 0.536" N, Long: 33° 6' 6.045" E, 3- Lat: 28° 58' 0.537" N, Long: 33° 6' 6.046" E, 4- Lat: 28° 59' 0.536" N, Long: 33° 7' 6.048" E, 5- Lat: 28° 59' 0.533" N, Long: 33° 7' 6.048" E and 6- Lat: 28° 59' 0.534" N and Long: 33° 9' 6.047" E as shown in Figure (1).

The available data in the considered area comprises of seismic and well-logs data.Four wells (RB-B11, RB-B13, RBA7 and RB-A10E)were made available within the study area. The well logs includeGamma Ray, Neutron, Density, Resistivity, Sonic, Dipmeter, and Spontaneous Potential logs. In addition to the vertical seismic profile that was used for identification of geologic tops and well correlation with surface seismic through a well-to-seismic tie.

Twenty (20) seismic lines from whichnine inline seismic lines conducted in the NE-SW direction (Inline-

145, Inline-155, Inline-165, Inline-175, Inline-185, Inline-195, Inline-205, Inline-215 and Inline-225) and another nine cross lines acquired in the NW-SE direction (crossline-229, crossline-244, crossline-259, crossline-274, crossline-289,crossline-304, crossline-319, crossline-334 and crossline-349). In addition to two composed lines in the NNE-SSW direction (composed Line-1) and in the ENE-SSW (composed Line-2) as shown in seismic lines and wells location map Figure (2).

PITFALLS OF RAS BUDRAN 3D PRE-STACK TIME MIGRATION (PSTM) SEISMIC SURVEY

The seismic survey was re-processed and produced PSTM cube in 1997 and the seismic image is mostlyof poor quality and the depth models of deep layers is often false due to the disturbed propagation of seismic energy through the deforming lens of the overlying layers. Therefore, it was quite challenging to be interpreted due to the following:

1. Small acoustic impedance contrast at all levels below top Rudeis.
2. Absorption of most of seismic energy (especially the high frequencies) at shallow evaporitic sequence.
3. Difficulties with effective multiple attenuation due to the thick sequences of interbedded shale, sands, salts, and anhydrates in the Miocene section.
4. Steep dipping overburden at the North West flank over the structure.
5. Complex intercepting fault pattern with transfer fault system

Main Seismic Data Processing Sequence

In (2010),CGG Veritas Company was contracted by Suez Oil Company (Suco) to carry out the processing of the PSTM to Pre-Stack Depth

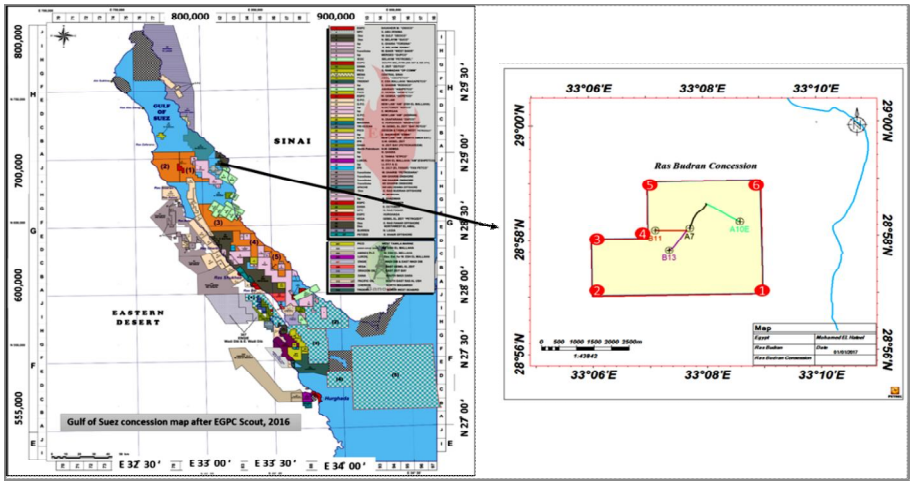

Figure (1): Location map of the study area.

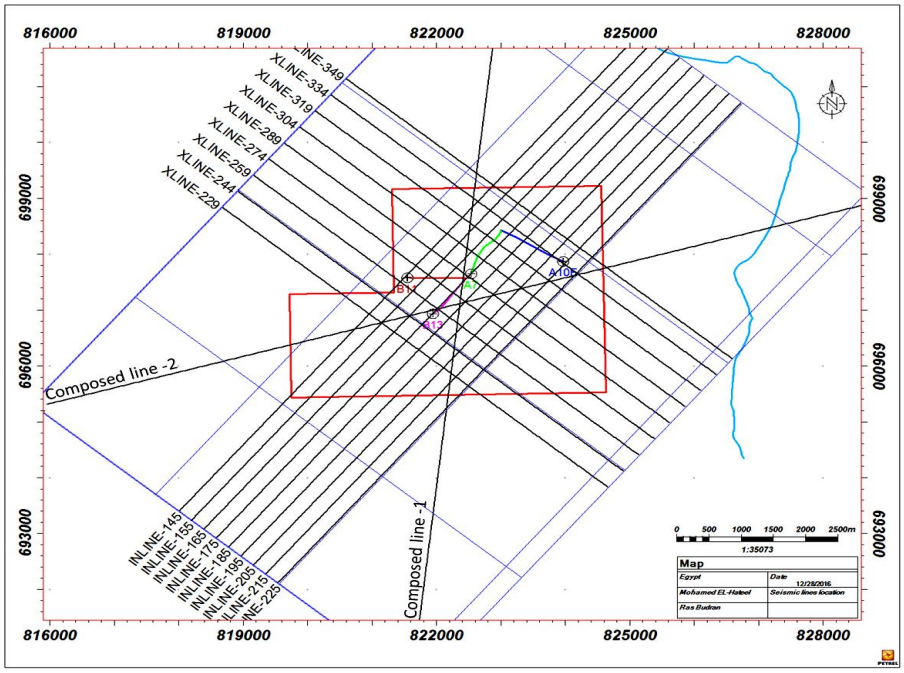

Figure (2): Seismic lines and boreholelocation map.

Migration (PSDM) to improve the subsurface image in the Pre-Miocene targets and improve the horizontal and vertical resolution of the data. Then, calibrate the PSDM volume with the drilled wells. Hence, the two surveys were re-processedover the study area as follows:

- The first data set is the streamer acquisition acquired in 1980 and covered the northern part of the RasBudran field.
- The second data set is the shallow water/transition Ocean Bottom Cable (OBC), 3D seismic survey acquired in 1997 and covered the southern part of the field.

Time processing data was processed with sample interval 4 ms and the record length was 5000 ms for OBC and 5120ms for streamer data set. Depth processing data was processed with sample interval 5 m and a record length of 10000 m.

Table (1): Streamer data set

Sail Line Re-Processing	
Processing Step	**Comments**
Reformat from SEGD to CGGVeritas internal format.	Record length 5120 ms, sample interval 4 ms.
Navigation seismic merge.	This required manual update of relation between field file number and shot point number On streamer grid.
Amplitude recovery	Time-gain correction $(T/250)^2$
HR – Radon for linear noise attenuation	1st pass (targeted for the first breaks.): Using CUT -700 ms 2nd pass (below direct arrivals to end of trace) Using CUT -850 ms
Frequency dependent noise attenuation	Attenuation of noise with frequencies from 34 to 46 Hz
Adaptive ground roll attenuation.	To remove low velocity aliased noise
Application start of data delay.	Start of data delay = 51.2 ms.
Application of gun static correction	Down shift 4.3 ms.
Shallow water de-multiple	Modeling and subtraction of multiple model
Deconvolution in TAUP domain	Using operator length of 240 ms and gap 36 ms.
Linear noise attenuation.	Application to remove velocities between 3500-5500 m/s over a frequency range of 3-30Hz, only in the affected areas.
Shot and channel amplitude corrections.	Filter length 41 in shot and channel directions.
Offset Class Processing	
Offset class sorting and 3D regularization.	Offset class definition is from 300-2600m, width 100m.
Streamer to OBC match	Applying phase rotation with angle -84, time shift 21018 micro second and time gain function on the streamer data.
Kirchhoff pre-stack time migration.	Aperture 4km, maximum dip 70 degree (T=0-2500ms), and 40 degree (T=3000ms- to the bottom).
CBM depth migration	Apertures 3.5km, maximum dip 60 degree.
CBM depth migration with swing attenuation	Apertures 3.5km, maximum dip 60 degree with swing attenuation of 15 degree below Kareem horizon and tolerance from 20 to 30 degree.
Post Time Imaging Processing	
Sort data into CDP gathers	Sort inline, crossline and offset.
High resolution Radon de-multiple.	Cut at maximum offset 240 ms.
Post Depth Imaging Processing	
Stretching data back to time	Using final depth velocity model to RL 5000 ms and SI 4 ms.
High resolution Radon de-multiple.	Cascaded cuts as following: •CUT of 280 ms at the maximum offset (2650 m) starting from 300 ms with time tapering of 500 ms. •CUT of 140 ms at the maximum offset (2650 m) starting from 2000 ms. •CUT of 120 ms at the maximum offset (2650 m) starting from 4000 ms.
25 degree mute and stack.	Raw stack.

Table (2): OBC data set

<table>
<tr><th colspan="2">OBC Re-Processing</th></tr>
<tr><th>Processing Step</th><th>Comments</th></tr>
<tr><td>Reformat from SEGD to CGGVeritas internal format.</td><td>Seismic and SPS data</td></tr>
<tr><td>Geometry update</td><td>SW 1: containing channel set configuration A
SW 2: containing channel set configuration B + C
SW 3: containing channel set configuration D
N.B. Receiver type not set in supplied rps file</td></tr>
<tr><td>Resample</td><td>From 2 ms to 4 ms using anti-alias filter</td></tr>
<tr><td>Application of digital filter delay.</td><td>Digital filter delay = 32 ms.</td></tr>
<tr><td>Low cut filter.</td><td>Butterworth filter 3Hz, 18dB/Oct.</td></tr>
<tr><td>Source matching</td><td>Match different source depths to the same average amplitude level</td></tr>
<tr><td>Geophone De-noise</td><td>
<table>
<tr><th>Processing</th><th>Comment</th></tr>
<tr><td>De-Spike</td><td>In order to remove high amplitude isolated spikes</td></tr>
<tr><td>Swell noise attenuation</td><td>2 passes of swell noise attenuation in shot point domain</td></tr>
<tr><td>Frequency dependent noise attenuation</td><td>Several passes to remove following frequency ranges:
60 – 75 Hz
80 – 90 Hz
40 – 50 Hz</td></tr>
<tr><td>adaptive ground roll attenuation</td><td>One pass</td></tr>
<tr><td>guided wave noise attenuation</td><td>One pass</td></tr>
</table>
</td></tr>
<tr><td>Hydrophone De-noise</td><td>
<table>
<tr><th>Processing</th><th>Comment</th></tr>
<tr><td>De-Spike</td><td>In order to remove high amplitude isolated spikes</td></tr>
<tr><td>Swell noise attenuation</td><td>2 passes of swell noise attenuation in shot point domain</td></tr>
<tr><td>Frequency dependent noise attenuation</td><td>Several passes to remove following frequency ranges:
60 – 75 Hz
80 – 90 Hz
40 – 50 Hz</td></tr>
<tr><td>Dispersive wave noise attenuation.</td><td>2 passes of dispersive noise attenuation to remove velocities between 800 - 1800 m/s over a frequency range of 3-45Hz</td></tr>
<tr><td>adaptive ground roll attenuation</td><td>Two passes</td></tr>
<tr><td>guided wave noise attenuation</td><td>One pass</td></tr>
</table>
</td></tr>
</table>

PZ Summation	**Summation using 5 points operator.**
De-noise post PZ summation	De-spike Swell noise attenuation. Frequency dependent noise attenuation. Radial trace mix for random noise attenuation.
De-bubble filter	Derived from modelled Pacific far field signature
Deconvolution	Surface consistent Deconvolution, with operator length of 240 ms and gap 36.
Surface consistent amplitude correction	Offset term.
zero phasing	Derived from modelled Pacific far field signature
Offset Class Processing	
Kirchhoff pre-stack time migration.	Aperture 4km, maximum dip 70 degree (T=0-2500ms), and 40 degree (T=3000ms- to the bottom)
Common offset vector (COV) Processing	
Sorting data into COV domain and regularization	Binning and regularizing the COV data (25x25)
CBM depth migration	Apertures 3.5km, maximum dip 60 degree.
CBM depth migration with swing attenuation	Apertures 3.5km, maximum dip 60 degree with swing attenuation of 15 degree below Kareem horizon and tolerance from 20 to 30 degree.
Post Time Imaging Processing	
Sort data into CDP gathers	Sort inline, crossline and offset.
High resolution Radon de-multiple.	CUT of 480 ms at the maximum offset.
Post Depth Imaging Processing	
Stretching data back to time	Using final depth velocity model to RL 5000 ms and SI 4 ms.
High resolution Radon de-multiple.	Cascaded cuts as following: •CUT of 640 ms at the maximum offset (6500 m) starting from 300 ms with time tapering of 500 ms. •CUT of 540 ms at the maximum offset (6500 m) starting from 1000 ms. •CUT of 480 ms at the maximum offset (6500 m) starting from 2000 ms. •CUT of 460 ms at the maximum offset (6500 m) ending at 5000 ms.
25 degree mute and stack.	Raw stack.

Table (3): Time VMB Re-Processing

Time VMB processing	
Processing Step	**Comments**
Applying matching filter	Matching between the two data set
Applying Pre-stack equalization (Pre-image)	Equalization pre image was applied using OPL 2000 ms
Migration for velocity picking	Every 50 meter by 50 meter.
Pre-conditioning for velocity picking	2 passes of HR Radon(1st pass with cutting parabola 320ms from top to bottom, the 2nd pass was using cutting parabola 200ms beginning from 3s followed by spectral offset balancing ended by adaptive AGC with OPL 2s.
Automatic velocity picking	RMO velocity picking
Migration velocity scans with 1Km grid for piking	The refrence for the scans was the RMO velocity the scans done (90-150%, step 5%)
velocity filtering	Velocity was smoothed using 5km radius

Table (4): Time merged volume Re-Processing

<table>
<tr><th colspan="2">Time merged volume</th></tr>
<tr><th>Processing Step</th><th>Comments</th></tr>
<tr><td>Generation of raw PSTM volume</td><td>Merging streamer and OBC data pre stack(OBC offsets limited to 3840m for this stack)</td></tr>
<tr><td>Post stack sequence volume - 1</td><td>- Post stack gapped de-convolution (gap 64ms, operator length 160ms).
- Coherency enhancement in the Tau-P domain.
- Adaptive equalization. (large sliding window 2000ms, small sliding window 500ms)</td></tr>
<tr><td>Post stack sequence volume - 2</td><td>- Post stack gapped de-convolution (gap 64ms, operator length 160ms).
- Coherency enhancement in the Tau-P domain.
- Adaptive equalization. (large sliding window 2000ms, small sliding window 500ms)
- Harsh Time variant filter:
<table>
<tr><th>Start time (ms)</th><th>End time (ms)</th><th>Frequency (Hz)</th><th>Slope (dB/Oct)</th><th>Frequency (Hz)</th><th>Slope (dB/Oct)</th></tr>
<tr><td>0000</td><td>0500</td><td>6</td><td>18</td><td>50</td><td>120</td></tr>
<tr><td>1000</td><td>1800</td><td>4</td><td>18</td><td>25</td><td>120</td></tr>
<tr><td>2000</td><td>3000</td><td>4</td><td>18</td><td>20</td><td>120</td></tr>
<tr><td>3400</td><td>6000</td><td>4</td><td>18</td><td>15</td><td>120</td></tr>
</table></td></tr>
<tr><td>Post stack sequence volume - 3</td><td>- Post stack gapped de-convolution (gap 64ms, operator length 160ms).
- Coherency enhancement in the Tau-P domain.
- Four passes of FK filter
- Adaptive equalization. (large sliding window 1000ms, small sliding window 200ms)</td></tr>
</table>

Table (5): Depth VMB Re-Processing

Depth VMB processing	
Processing Step	**Comments**
Streamer data	
Pre conditioning	Applying phase rotation with angle -84, time shift 21018 micro second and time gain function on the streamer data. – As applied for PSTM data.
First pass of velocity update	
CBM for RMO picking	On grid 50 by 50 meter
Pre-conditioning of RMO picking (in depth)	High resolution Radon de-multiple with cut of 280ms at maximum offset
Second pass of velocity update	
CBM for RMO picking	On grid 50 by 50 meter
Pre-conditioning of RMO picking (in depth)	High resolution Radon de-multiple with cut of 280ms at maximum offset
OBC Data	
COV sorting	Sorting the data to common offset vector domain
regularization	Binning and regularizing the COV data (25x25)
First pass of velocity update	
CBM for RMO picking	On grid 50 by 50 meter
Stretching data to time	Data was stretched to time using MBU0_1 as velocity function for stretching
Pre-conditioning of RMO picking (in time)	High resolution Radon de-multiple with cut of 400ms at maximum offset.
Stretching to depth	Stretching the data back to depth using MBU0_1
Second pass of velocity update	
CBM for RMO picking	On grid 50 by 50 meter
Stretching data to time	Data was stretched to time using MBU0_1 as velocity function for stretching
Pre-conditioning of RMO picking (in time)	High resolution Radon de-multiple with cut of 400ms at maximum offset.
Stretching to depth	Stretching the data back to depth using MBU0_1
Velocity	
Smoothing PSTM velocity	2km smoothing in inline and crossline direction and 100ms smoothing operator from top to 2500ms, then 200ms smoothing operator from 3000ms to the bottom
DIX conversion	Converting the VRMS to interval velocity
Stretching to depth	Stretching the interval velocity in time into depth with record length 11 km

Smoothing vint in depth	dx,dy 4km, and 400ms vertically from top to bottom (MBU01) Clipping the high velocity at maximum velocity 5000m/s (MBU-02) Clipping the high velocity using iso-surface velocity of 4500m/s ending the model with velocity 4900m/s. (MBU-03) Scaling and smoothing the MBU01 to match the interval velocity of the check shot profile (MBU04)
Defining water layer velocity	Scans were done (1460-1520m/sec) to insert the proper water velocity
Initial velocity model MBU05	It is a merged velocity model between MBU01 & MBU04
Shallow isotropic velocity model update	2 iterations MBU110, and MBU113 (B-spline 250x250x70m for both)
Incorporation of low velocity layer	MBU213
Migration scans for structural picking in deep below Kareem horizon	Scan velocity for picking from 85% to 105% with increment 5 % in the cross line direction.

Table (6): CBM depth merged volume Re-Processing

Post Imaging Processing	
Processing Step	**Comments**
Post stack merge	Generate raw stack
Post stack processing sequence -1	3D FK footprint removal. Coherency enhancement filtering Butterworth frequency filtering (as applied on the PSTM volume) Whitening to 35Hz maximum frequency.
Post stack processing sequence -2	3D FK footprint removal FK filter for dip removal (as applied on the PSTM volume) Coherency enhancement filtering Butterworth frequency filtering (as applied on the PSTM volume) Whitening to 35Hz maximum frequency.

Table (7): Swing attenuation CBM depth merged volume Re-Processing

Post Imaging Processing	
Processing Step	**Comments**
Post stack merge	Generate raw stack
Post stack processing sequence	3D FK footprint removal. Coherency enhancement filtering Butterworth frequency filtering (as applied on the PSTM volume) Whitening to 35Hz maximum frequency.

Velocity Model Building

1) PSTM velocity model building

a) PSTM velocity analysis

Similar to the 1 by 1 km velocity analysis, the PSTM velocity analysis was carried out on both data sets; streamer and OBC after matching streamer to OBC data in order to derive both velocity field and anisotropic parameters to be used for the anisotropic Kirchhoff PSTM. Velocity analysis was carried out on migrated Pre-STM gathers of 50 m by 50 m grid. A mild radon De-multiple was applied prior to the analysis.

The PSTM data was migrated using the velocity fields picked in the 2nd pass of velocity step. Deriving velocity fields on data that has undergone PSTM ensures data is picked for velocities in its "migrated" position. This removes discrepancies in conflicting dips during the analysis (primaries and diffractions).

The PSTM velocity analysis was carried out using CGGV's High Density Anisotropic Velocity Analysis (HDPIC) module. This module is an automated velocity analysis tool that picks both $V_{rms}$and Effective Transverse Anizotropy(ETA). A reliable reference velocity function is required to drive the HDPIC analysis. This reference velocity field driving the HDPIC was the velocity fields picked in the 2nd pass of velocity analysis. The velocity field was Quality controlled (QC'd) by reviewing the interval and RMS velocities and in the in-line and crossline (IL/XL).

The crossline view was used to check the velocities being picked consistently along one crossline passing through both data sets and that no anomalous picks were made. Also the Automatic PSTM velocity analysis had been modified and QC'd by output the migration scans every 1 km in the crossline direction.

This scans were run from 90% up to 105% in steps of 5% with the fourth order field held constant. The output gathers were muted to 30º and the velocity crossline was stacked. After structural velocity picking the velocity was smoothed using 5km operator.

b) Kirchhoff PSTM production

Kirchhoff PSTM was used. Kirchhoff migration is an imaging tool that is basically suited for moderately complex geology. The technique is suitable for steep dip imaging and produces AVO-friendly common-image-gathers in the offset domain. Thismethod uses pre-computed travel time maps from surface positions to a regular 3D grid in the subsurface to migrate the recorded data traces into the time or depth space (Hill, 2001; Gray et al., 2002; Notfors et al., 2006; Sun et al., 2007; Roberts et al., 2008 and Vinje, 2008).

Maximum one travel time (corresponding to one ray-path) is calculated from each point at the surface to each point in the subsurface. This travel time may correspond to the ray with the shortest travel time, the largest energy, or the shortest ray-path. Both streamer and OBC migrated separately in offset classes and then merged afterword. A diffracted aperture 4.0 km with dip limit 70 degree from the water bottom to time 2500 ms and dip limit 40 degree from time 3000 ms to the end of trace.

2. PSDM velocity model building

a) Generation of initial velocity model

The initial velocity model was created using the PSTM time imaging velocity field. This was converted from a time RMS velocity field to a depth interval velocity field by a 1D Dix conversion. Prior to conversion the model was smoothed. After which 4000 m and 400 m filtering were applied to the interval velocity in the depth domain. Also, different initial velocity models were generated and tested (Figure 3).

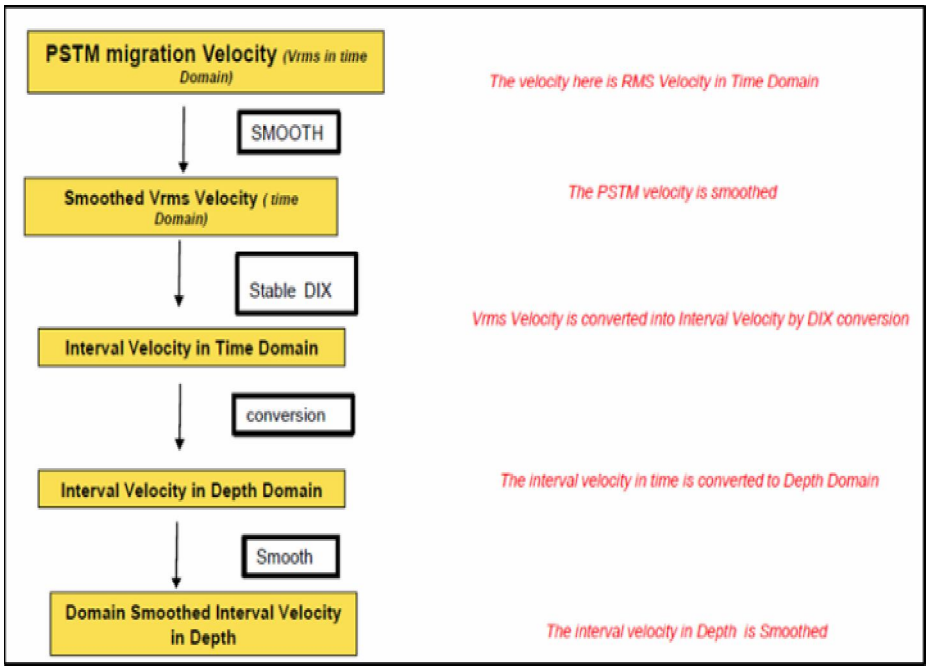

Figure (3): Overview of initial velocity model.

Figure (4) shows good comparison of velocity models in both time and depth migration where the time migration with no lateral velocity changes are comprehended and the ray path is always symmetric about a zero offset trace.While the depth migration comprehends velocity changes vertically and laterally and the ray path is non-symmetric about a zero offset trace.

velocity models.

Figure (5) illustrates interval velocity slice of the CBM 3D PSDM in depth domain at depth of 3030 m with a high lateral velocity change at target depth.

Figure (6) shows how the reliable velocity model captures the heterogeneity as well as illuminates the sub-salt complexgeologic structure of the crossline 289 seismic section within the study area.

b) Final Controlled Beam PSDM

Controlled Beam Migration (CBM) is a specialized version of Beam migration designed to achieve improved signal-to-noise ratios and steep dip imaging in complex geological settings (Gray et al., 2002).

The data was imaged using CGG Veritas controlled beam PSDM algorithm which combines the steep-dip imaging capabilities of Kirchhoff techniques with the multi-arrival abilities of wave-equation migration.

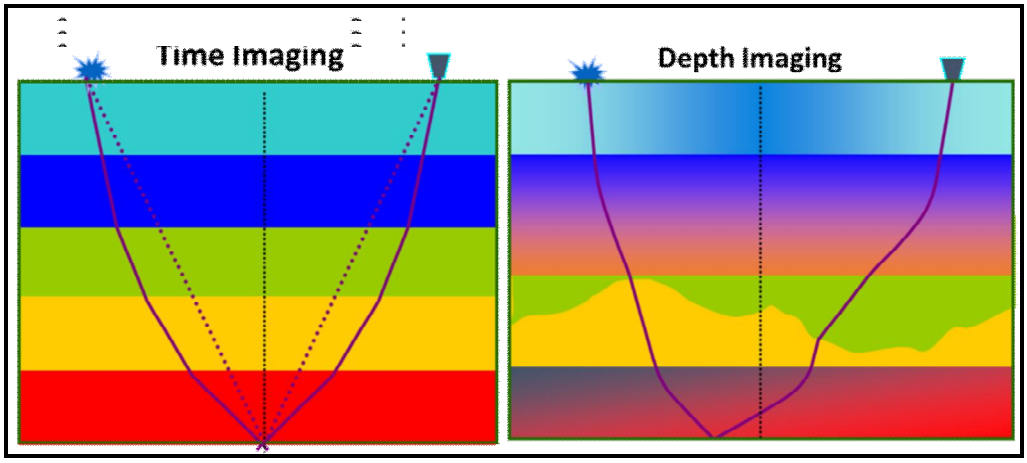

Figure (4): Comparison between time and depth.

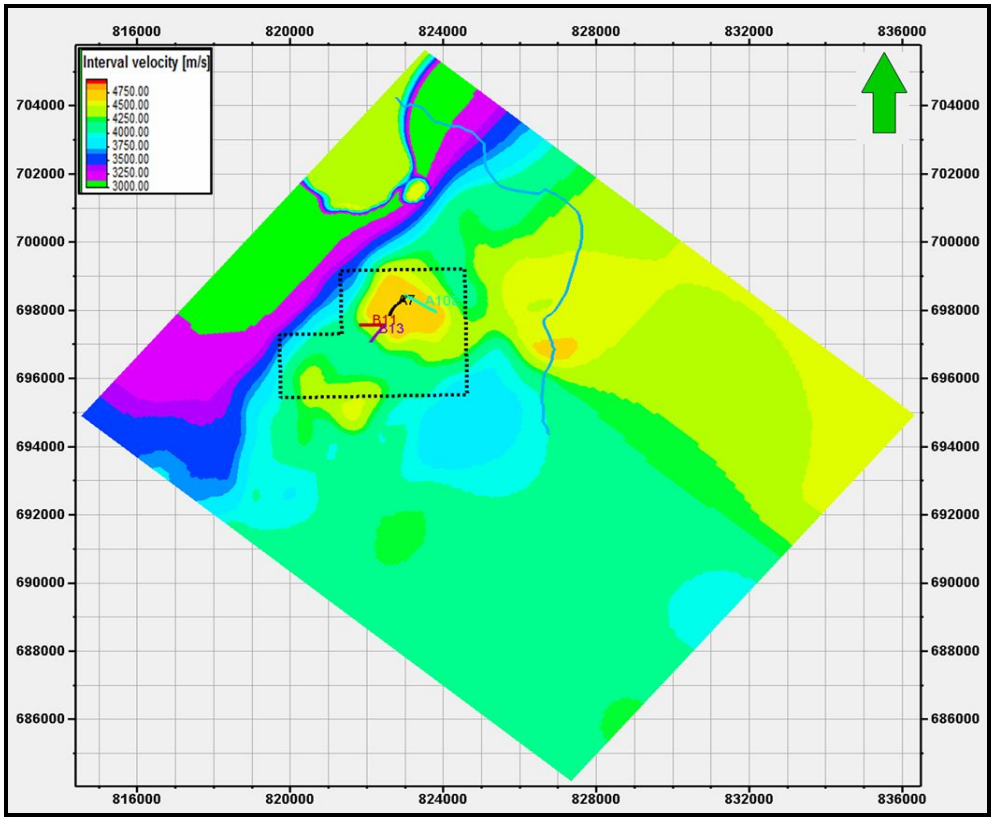

Figure (5): Depth interval velocity slice of the CBM 3D PSDM at depth of 3030 m showsa high lateral velocity change at target depth.

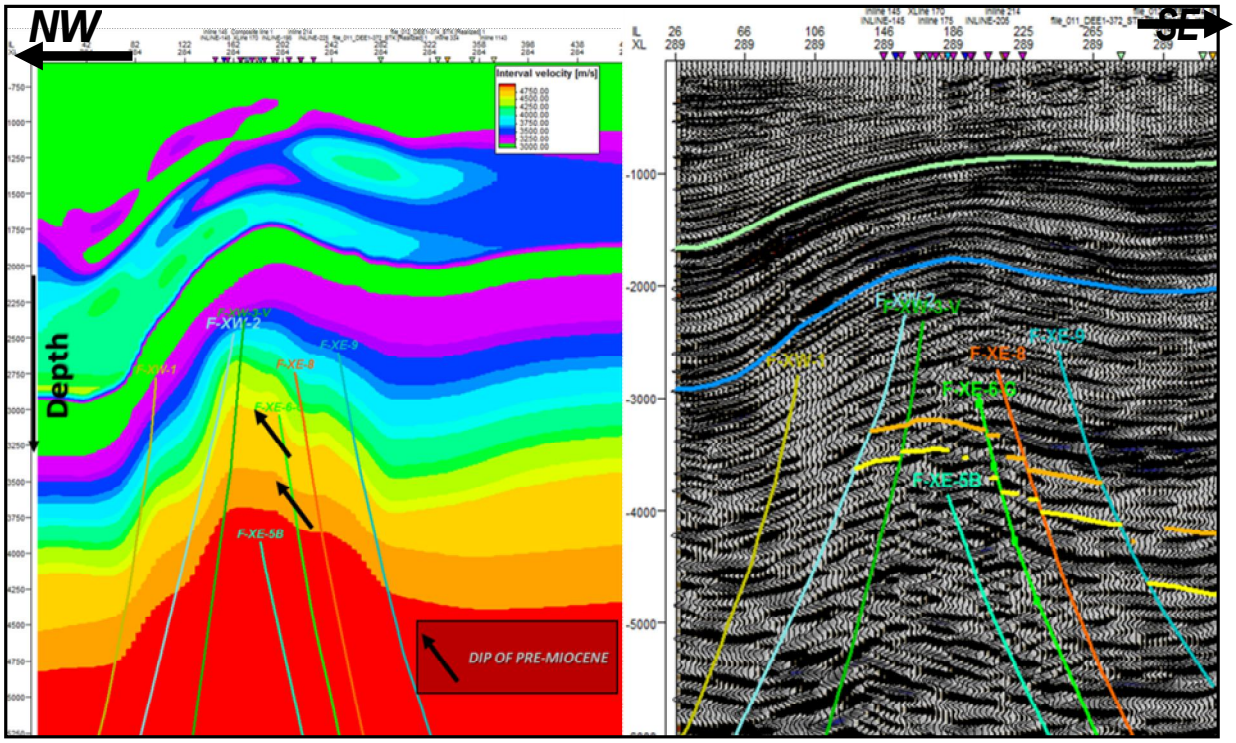

Figure (6): Reliable velocity model (left) of the CBM 3D PSDM crossline 289 seismic section (right) declares the velocity heterogeneity and enhances the sub-salt complex structure.

CGGVeritas implemented beam migration (Gray et al., 2002) and wasused extensively as imaging tool for areas of complex structure (Notfors et al., 2006; Sun et al., 2007; Roberts et al., 2008). Recent further development of the method resulted in an enhanced version known as controlled beam migration (CBM), a useful and valuable addition to the depth imaging toolbox.

BENEFITS OF CONTROLLED BEAM MIGRATION (CBM) ALGORITHM OF THE PSDM

1- Improve signal-to-noise ratio, especially in sparse, low-fold land and OBC data.
2- It is a powerful and useful tool enabling enhanced structural interpretation.
3- Enhance sub-salt image.
4- Enhance salt flank and base imaging.
5- Improve steep dips in complex geologic section.
6- Accelerate velocity model building in complex areas such as sub-salt. With its ability to image structures such as over thrusts and basement fractures the technique is valuable tool for accurate mapping of complex geology.
7- Controlled Beam Migration would appear to offer the best of both the Kirchhoff and One-Way Wave Equation Worlds.
8- Attenuate diffraction noises
9- Finally, multiple attenuation option has been added to CBM which allows discriminating internal multiples. This confirmed to be useful particularly in areas such as the shallow part of the geologic section in RasBudran oil field.

Prior to running this methodology, both the dip limit and aperture were tested to be used for the migration. Aperture of 3500 m, 4000 m and 4500 m were tested with a dip limit of 70°. An aperture of 4000 m was selected and used for tests of the dip limit. Dip limits of 40°, 50°, 60°, 70° and 80° were then tested. A dip of 60° and an aperture of 3500 m were selected for the production migration for both standard and swing attenuation CBM. Finally the volume PSDM production used the following parameters:

Output Depth	10000 m
Output Sampling	5 m
Input bin size	25.0 m x 25.0 m
Output bin size	25.0 m x 25.0 m
Migration aperture	3500 m x 3500 m
Dip Limitation	60 degree
Anti-alias filter	37.50 x 37.50 m

We willdemonstratethe benefits of CBM with a selection of examples fromRasBudran oil field inthe central part of the Gulf of Suez which ranges from the re-processing oflegacy data to complex PSDM velocity model building.

APPLICATIONS OF THE CONTROLLED BEAM MIGRATION –RAS BUDRAN FIELD

Beam migration has been used extensively around the worldby CGGVeritas to address a variety of imaging challenges:

Example 1: Improvement of signal-to-noise ratio

The first example demonstrating how the Controlled Beam Migration improves the depth imagingin the presence of large velocity contrasts, where multi-pathis likely to occurasillustratedininline 175 seismic section.

The Kirchhoffimage (left) is contaminated withmigration smiles, rise times artifacts and multiple arrivals of the ray paths at the base of salt resulting in noisy image qualityat Miocene section as shown in left side of Figure (7).

The Controlled Beam Migration (right)revealed the enhancementofthe seismic image at both Miocene and pre-Miocene levels which assure better imaging than the Kirchhoff methodology.

Example 2: Enhancement of sub-salt structural features

The CBM has improved the subsalt imaging and complex structure and preciselydefined the fault pattern both the NW-SE and NE-SW directions as shown in figures 8 and 9.

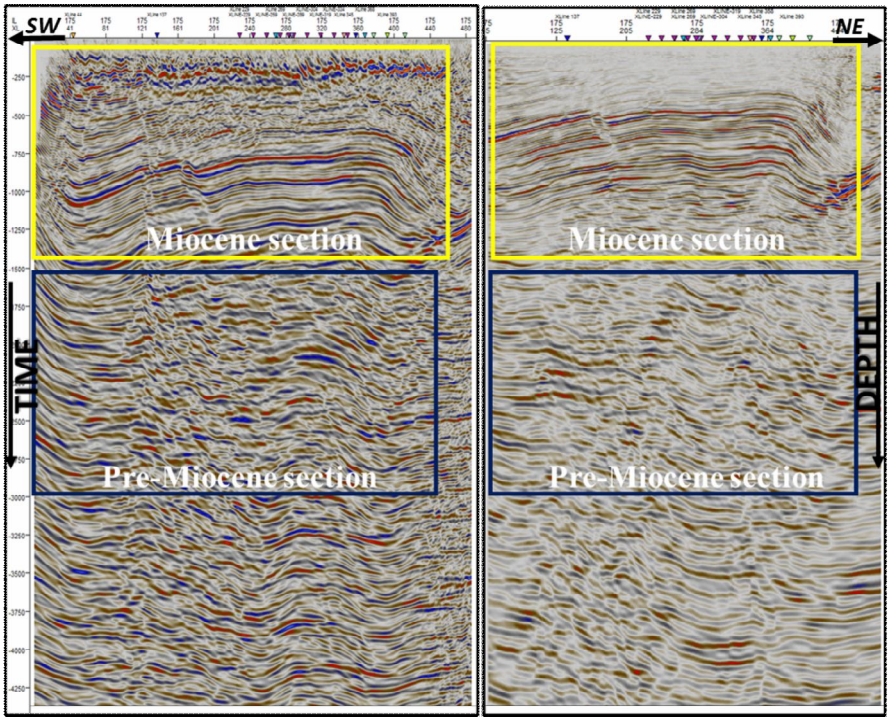

Figure (7): 3D seismic section crossline 175 at RasBudran Kirchhoff PSTM migration(left) and controlled beam migration PSDM (right).

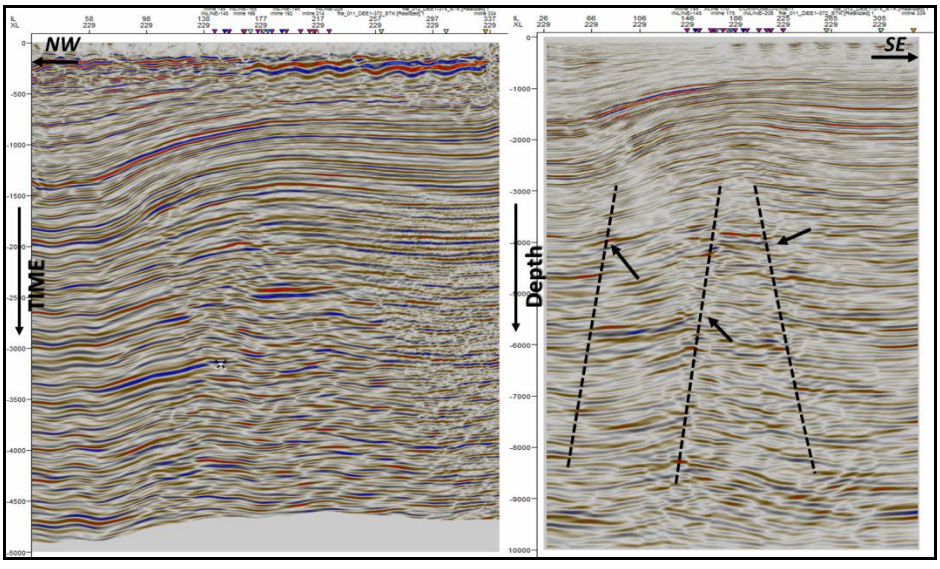

Figure (8): 3D seismic section crossline 229 inRasBudran Kirchhoff PSTM migration (left) and controlled beam migration PSDM (right) with better transfer fault detection in the NE-SW direction.

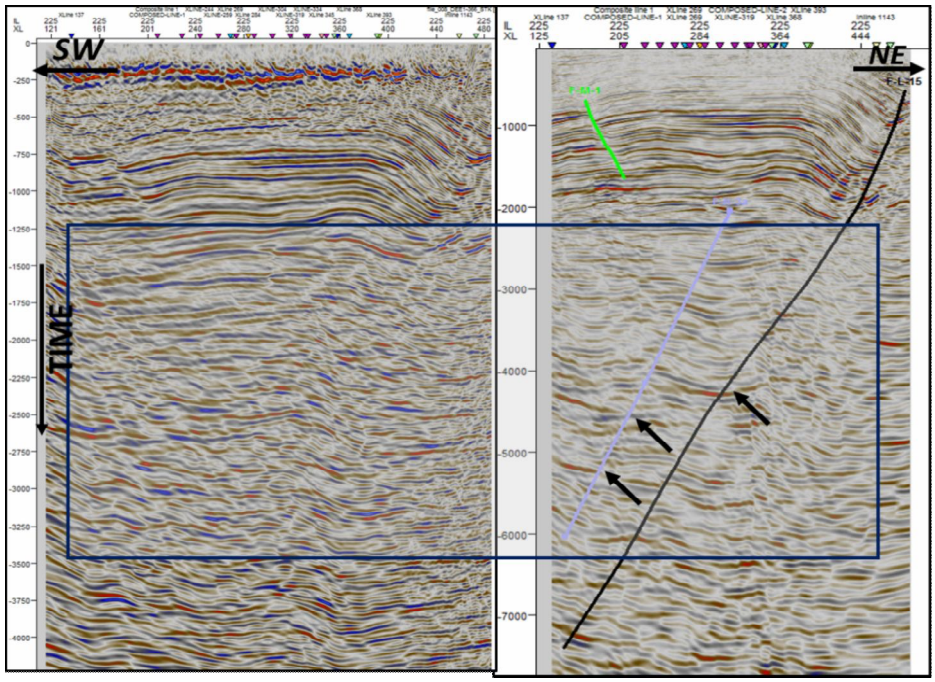

Figure (9): 3D seismic section inline 225 inRasBudran Kirchhoff PSTM migration (left) and controlled beam migration PSDM (right) with better Clysmic fault detection in the NW-SE direction.

Example 3: Attenuation of diffraction noise and tracking reflection continuity

Figure (10) shows a 3D seismic section inline 319in RasBudran Kirchhoff PSTM migration (left) before diffraction attenuation and a controlled beam migration PSDM (right) after diffraction removal enabling a good tracking of the continuity of the pre-salt reflection horizons.

Example 4: Improvement of steep dips in complex geologic section.

Figure (11) shows a 3D seismic section inline 175 inRasBudran Kirchhoff PSTM migration (left) before improvement of the steep dips in the complex pre-Miocene section and indicates false dips in the NW direction, while the controlled beam migration PSDM (right) improves the steep dips in their correct direction in the NE direction that is confirmed by the actual dipmeter data and FMI image of the drilled well RB-B13.

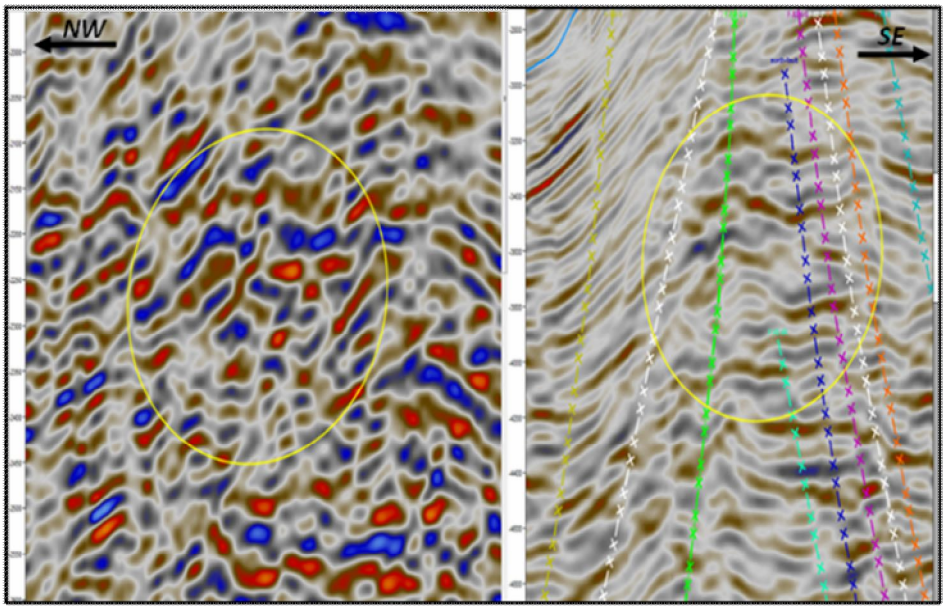

Figure (10): 3D seismic section inline 319inRasBudran Kirchhoff PSTM migration (left) and controlled beam migration PSDM (right) with diffraction attenuation and good reflection horizon continuity.

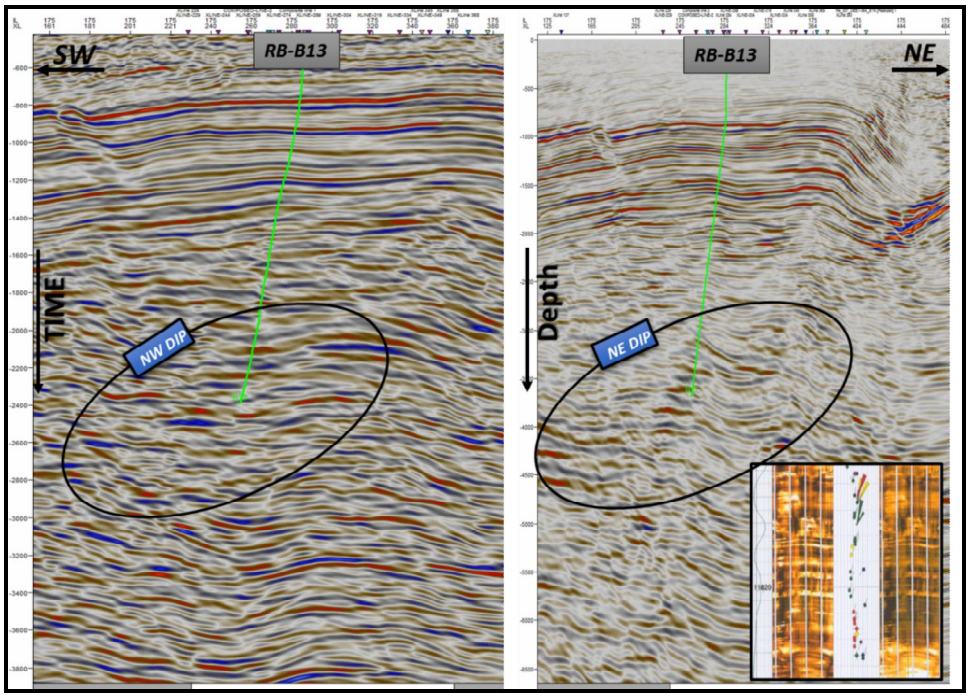

Figure (11): 3D seismic section inline 175inRasBudran Kirchhoff PSTM migration (left) with false NW dip direction,controlled beam migration PSDM, dipmeter and FMI image (right) with correct NE dip direction.

SUMMARY AND CONCLUSIONS

Controlled Beam Migration is an efficient, flexibleand powerful family of migration techniques. It can provide cleaner imageswithout suffering from the single arrival limitation of Kirchhoff or the diplimitationsof one-way wave-equation migration.

Controlled Beam Migration enhances the image-signalto-noise,steep dips anddelivers clear easy-to-interpret structural images in complex areas and build correct velocity models.

The present study enhances the depth imaging of the deep structural objectives beneath a complex overburden that may show strong horizontal and vertical velocity variations.

In this paper, we have presented several examples after applying this powerful technique enhancing the sub-salt depth imaging, improve signal-to-noise ratio, enhancing structural interpretation, improve steep dips in complex geologic section, building reliable velocity models, attenuate diffraction noises and finally, attenuating multiple reflections of several orders.

REFERENCES

Gray, S., Notfors, C., and Bleistein, N. (2002): Imaging using multi-arrivals: Gaussian beams or multi-arrival Kirchhoff, SEG 72nd International Meeting, Expanded Abstracts, 21, 1, 1117-1120.

Hill, N.R. (2001): Prestack Gaussian beam depth migration. *Geophysics*, 66, 1240-1250.

Notfors, C., Xie, Y. and Gray, S. (2006): Gaussian beam migration: a viable alternative to Kirchhoff. *EAGE 65*th *Conference &Exhibition*, Extended Abstracts, G046.

Roberts, G., Leggott, R., Wombell, R. and Williams, G. (2008): Beam migration in the North Sea. *Norwegian Petroleum Society Biennial Geophysical Seminar*, Kristiansand.

Sun, J., Don, P., Tang, Q., Bone, G. and Giang, N.T. (2007): Imaging of fractures and faults inside granite basement using controlled beam migration. *ASEG 19*th *International Geophysical Conference & Exhibition.*

Vinje, V., Roberts, G., and Taylor, R., (2008): Controlled beam migration: a versatile structural imaging tool, EAGE, first break, 26, 109-113.